

Dynamics of Crystal Formation in the Greenland NorthGRIP Ice Core

Joachim Mathiesen, Jesper Ferkinghoff-Borg, Mogens

H. Jensen, Mogens Levinsen, and Poul Olesen

The Niels Bohr Institute, Blegdamsvej 17, DK-2100 Copenhagen, Denmark.

Dorthe Dahl-Jensen and Anders Svensson

*Department of Geophysics, The Niels Bohr Institute for Astronomy, Geophysics,
and Physics, Juliane Maries Vej 30, DK-2100 Copenhagen, Denmark.*

The North Greenland Ice Core Project (NorthGRIP) provides paleoclimatic information back to at about 120 kyr before present (Dahl-Jensen and others, 2002). Each year, precipitation on the ice sheet covers it with a new layer of snow, which gradually transforms into ice crystals as the layer sinks into the ice sheet. The size distribution of ice crystals has been measured at selected depths in the upper 880 m of the NorthGRIP ice core (Svensson and others, 2003b), which covers a time span of 5300 years. The distributions change with time toward a universal curve, indicating a common underlying physical process in the formation of crystals. We identify this process as an interplay between fragmentation of the crystals and diffusion of their grain boundaries. The process is described by a two-parameter differential equation to which we obtain the exact solution. The solution is in excellent agreement with the experimentally observed distributions.

The NorthGRIP drilling location (75.10 N, 42.32 W) is situated on an ice ridge with an ice thickness of 3085 m. The mean annual temperature is -32 deg. Celsius and the annual accumulation in the area is on the average 19.5 cm ice equivalent. In the upper 80 m of the ice sheet, the firn, the snow gradually compacts to a close packing of ice crystals of typical sizes 1 to 5 mm. We apply crystal size distributions obtained from fifteen vertical thin sections of ice evenly distributed in the depth interval 115 - 880 m (Svensson and others, 2003b). The thin sections have dimensions of 20 cm \times 10 cm (height \times width) and a thickness of 0.4 ± 0.1 mm.

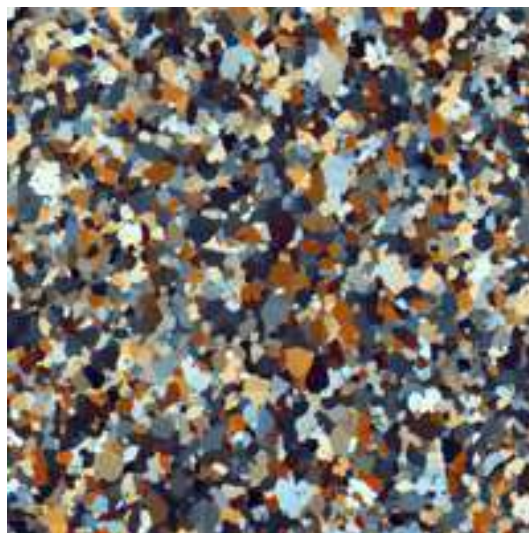


FIG. 1: An image of a 10 x 10 cm² vertical thin section of ice from the depth 115 m. The section is viewed between two crossed linear polarizers and the different colors represent almost 3000 individual crystals with various orientations of the crystal optical c-axes.

Digital images of ice thin sections placed between crossed linear polarizers have been used to map the dimensions of individual ice crystals in the sample (Fig. 1). The ages of the considered samples are all less than 5300 years (Johnsen and others, 2001), and the temperature of the ice in this period can be assumed constant (Dahl-Jensen and others, 1998).

Fig. 2 shows size distributions of ice crystals at selected depths down to 880 m (5300 years before present (B.P.)). The crystal size is defined as the vertical extent of a crystal, which is estimated as the height of the minimal and vertical aligned rectangle, which encloses the individual crystal. Using the horizontally measured sizes of the ice crystals from the thin

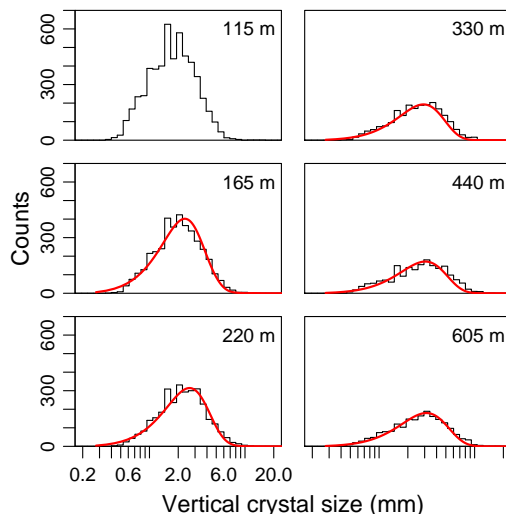


FIG. 2: Distributions of ice crystal sizes at depths 115m, 165m, 220m, 330m, 440m and 605m. The crystal size is defined as the maximum vertical extent of the individual crystals. The black lines are the measured histograms and the smooth lines are the temporal evolution predicted by eq. (2) starting from the initial distribution at 115m. The total counts of ice crystals decreases with depth (due to the overall increase of sizes) until the steady state is reached.

sections, one obtains similar distributions. The thin sections used in determining the ice size distributions have typical thicknesses of 0.4 ± 0.1 mm, and ice crystals with all length scales smaller than this thickness will consequently be either smoothed away when cutting the ice or be invisible when viewed in the linear polarizers. These small crystals will be seen as part of the larger crystals and not as individual crystals. This corresponds to an average increase in the sizes of the large crystals, i.e. the lengths we measure x are equal to the real length \hat{x} plus some noise ϵ of positive mean, $x = \hat{x} + \epsilon$. We have assumed that this noise is sufficiently peaked around half the thickness of the thin section, such that we simply put $\epsilon = 0.2$ mm. This value of ϵ has been used in the comparisons between theoretical and experimental values.

Each distribution exhibits a pronounced peak, indicating a typical crystal size at each depth, followed by an exponentially decaying tail of relatively large crystals. The mean size becomes larger with depth and thus time until it reaches a limiting crystal size (Thorsteinsson and others, 1997; Li and others, 1998). The most important physical process behind such growth is diffusion of grain boundaries between the ice crystals. Inhomogeneities on the

crystal boundaries, characterized by small radii of curvature, tend to be smoothed out as time progresses. This causes the inhomogeneities to be incorporated into the larger crystals leading to an overall growth of the mean crystal size (Alley and others, 1986; Paterson, 1994). This approximative description leads to the so-called Normal Grain Growth law that predicts the following temporal dependence of the mean crystal size x ,

$$\langle x^2 \rangle(t) = x_0^2 + kt, \quad (1)$$

where x_0 is the initial mean crystal size and k is the crystal growth rate. This approach was successfully applied for the GRIP ice core by Thorsteinsson and others, 1997, who fitted their experimental observations well back to 2500 B.P. By definition, however, the diffusion does not cause the crystal size to reach a limiting size, which is in disagreement with the actual observations that clearly indicates a saturation in $\langle x^2 \rangle$ after 2500 B.P. (Alley and Woods, 1996; Gow and others, 1997; Thorsteinsson and others, 1997).

The important missing part of the physical mechanism in this model is the fact that all crystals, and in particular the large ones, are subjected to fragmentation processes or - as often referred to in ice physics - polygonization or rotation recrystallization (Alley and others, 1995; Thorsteinsson et al., 1997). We here include this process in the description which then leads to a physical model with a balance between the diffusion of grain boundaries and the fragmentation of crystals causing the mean crystal size to reach a steady state after 2500 B.P.

Another process that has been proposed as important for the production of small crystals is nucleation, or the formation of new grains, which may have c-axis orientations that differ from the dominating vertical orientation of the surrounding crystals. Measurements of the NorthGRIP fabric (c-axis orientations) suggest, however, that nucleation does not seem to play an important role in the Holocene (Wang and others, 2002; Svensson and others, 2003b), and nucleation is not included in the model.

Our proposed model is formulated as a rate equation in the quantity $N(x, t)$, which is the density of ice crystals of length x at time t measured B.P. In this study x is chosen as the vertical extent of the crystals. At a given time, $N(x, t)$ can be increased or decreased by diffusion with a diffusion constant D . It can receive fragments of size x from fragmentations of larger crystals and it can decrease by its own fragmentation. The fragmentation is defined as a rate f in length and time, i.e. for a given time step dt the average number of

fragmentation events over a length L is $fLdt$.

The fragmentation rate f , and the diffusion constant D , will depend on temperature, non-hydrostatic stresses in the ice and moreover be sensitive to the impurity content of the ice (Alley and others, 1986).

These diffusion and fragmentation processes lead to an integral-differential equation on the form

$$\frac{\partial N(x, t)}{\partial t} = D \frac{\partial^2 N(x, t)}{\partial x^2} - fxN(x, t) + 2f \int_x^\infty N(x', t) dx' \quad (2)$$

Here, the first term on the right hand side is a diffusion term that corresponds to the grain boundary diffusion of the Normal Grain Growth law, i.e. if we only include this term in the model we reproduce for large times the parabolic behavior in (1). Note that the equation describes the dynamics of the full assembly of crystals and that the mean square of the crystal sizes therefore follows from

$$\langle x^2 \rangle(t) = \int_0^\infty x^2 N(x, t) dx / \left(\int_0^\infty N(x, t) dx \right). \quad (3)$$

If we only include the diffusion term in eq. (2), we get for large times that $\langle x^2 \rangle(t) \sim 4Dt$. The behavior at large times differs from normal diffusion by a factor of two because we use the absorbing boundary condition that for all times $N(0, t) = 0$.

The last term in (2) is the contribution from fragmentation of larger crystals into crystals of size x . Combining the two ways a crystal of size $x' > x$ can produce a fragment of size x with the assumption that there is a uniform probability, $1/x'$ for where the crystal break, we get

$$fx'N(x') \cdot \frac{2}{x'}, \quad (4)$$

where $fx'N(x')$ is the number of crystals of size x' that fragments per time and $2/x'$ is the probability for generating a fragment of size x . Note that the assumption of a uniform probability already was made in the definition of the rate f . If we integrate (4) over all crystals larger than x we achieve the last term in (2).

Dividing through by f in eq. (2), we obtain an expression on the right hand side which depends on one parameter $a = D/f$ only. The integral-differential equation has analytic solutions, $B\left(\frac{x+\lambda}{a^{1/3}}\right)$, which are explicitly given in terms of the Bessel function $K_{\frac{1}{3}}$ and eigenvalues λ ,

$$B\left(\frac{x+\lambda}{a^{1/3}}\right) = \frac{x^{3/2}}{\sqrt{3}} K_{\frac{1}{3}}\left(\frac{2}{3}\left(\frac{x+\lambda}{a^{1/3}}\right)^{3/2}\right). \quad (5)$$

The function $K_{\frac{1}{3}}(x)$ can be written as a sum of the more frequently used Bessel functions $I(x)$, $K_{\frac{1}{3}}(x) = \frac{\pi}{\sqrt{3}}(I_{-\frac{1}{3}}(x) - I_{\frac{1}{3}}(x))$. The boundary condition, $N(0, t) = 0$ for all times t , implies that only a discrete set of non-positive values for λ is allowed. They are found by solving the equation $B\left(\frac{\lambda}{a^{1/3}}\right) = 0$. The largest eigenvalues are $\lambda_0/a^{1/3} = 0$, $\lambda_1/a^{1/3} = -2.338\dots$, $\lambda_2/a^{1/3} = -4.088\dots, \dots$. The general solution can be written as a linear combination of the eigenfunctions,

$$N(x, t) = \sum_{n=0}^{\infty} c_n B\left(\frac{x + \lambda_n}{a^{1/3}}\right) e^{\lambda_n f(t-t_0)} \quad (6)$$

where the c_n 's can be computed from the distribution at time $t = t_0$ (for further details see the work of (Ferkinghoff-Borg and others, 2003)). The fact that we have no positive eigenvalues guarantees the existence of a steady state solution, which is defined by the only surviving term (corresponding to $\lambda_0 = 0$) for high ages,

$$N(x, t) \sim B(x/a^{1/3}) \quad \text{for } t \rightarrow \infty. \quad (7)$$

The characteristic time, τ , of the exponential growth towards steady state is given by the second largest eigenvalue, λ_1 , i.e.

$$\tau = -1/(\lambda_1 f) \approx (2.338 \cdot f \cdot a^{1/3})^{-1}.$$

When the dynamics has reached steady state, and the mean crystal size has saturated, the distribution is described by the single parameter, $a^{1/3}$, which defines the characteristic length scale of the system. In particular, one finds that the mean vertical size in the steady state is

$$\langle x \rangle_{\infty} = 3^{2/3} \frac{\Gamma(4/3)}{\Gamma(3/2)} a^{1/3}.$$

In Fig. 3 we show the mean vertical size of the ice crystals, $\langle x \rangle(t)$ as function of time. The dots are the experimental values and the solid line is an exponential fit corresponding to the two leading terms in the solution,

$$\frac{\langle x \rangle_{\infty}}{1 + \left(\frac{\langle x \rangle_{\infty}}{\langle x \rangle_0} - 1\right) e^{-(t-t_0)/\tau}}, \quad (8)$$

where $\langle x \rangle_0$ is the observed average length at time $t_0 = 500$ years. From the figure, we estimate the characteristic time, $\tau = 600 \pm 70$ years and the average length in the steady state $\langle x \rangle_{\infty} = 2.9 \pm 0.1$ mm. The two parameters correspond to an effective fragmentation rate and

a diffusion constant of respectively $f = (5.2 \pm 0.6) \cdot 10^{-4} \text{ mm}^{-1} \cdot \text{yr}^{-1}$ and $D = (1.4 \pm 0.2) \cdot 10^{-3} \text{ mm}^2 \text{yr}^{-1}$. Following eq. (3) we obtain the Normal Grain Growth crystal growth rate $k = 4D = (5.5 \pm 0.8) \cdot 10^{-3} \text{ mm}^2 \text{yr}^{-1}$, which corresponds very well with the known values for GRIP, $k = 5.6 \cdot 10^{-3} \text{ mm}^2 \text{yr}^{-1}$ (Thorsteinsson and others, 1997), and for NorthGRIP, $k = 5.8 \cdot 10^{-3} \text{ mm}^2 \text{yr}^{-1}$ (Svensson and others, 2003b). In this work we are using the maximum vertical extent of the crystals, so that no correction value for the sectioning effect is needed.

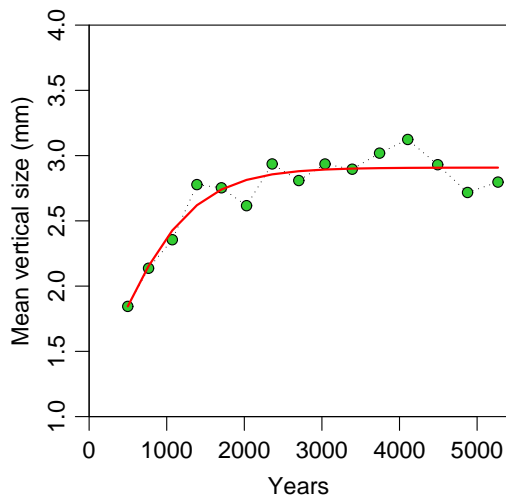


FIG. 3: The mean vertical size of the ice crystals shown versus their age in years B.P. The smooth line shows the best fit predicted from our dynamical description of ice crystal growth. From the fit we read off the diffusion constant, $D \approx 1.4 \cdot 10^{-3} \text{ mm}^2 \cdot \text{yr}^{-1}$, and fragmentation rate, $f \approx 5.2 \cdot 10^{-4} \text{ yr}^{-1} \cdot \text{mm}^{-1}$. The time scale is taken from ref. (Johnsen and others, 2001).

Using these estimates, we can predict the time evolution of crystal sizes from any initial distribution. The solid lines in Fig. 2 show the time evolution of the distribution observed at time $t_0 = 500$ years (115 m depth), in good agreement with the experimental results.

When comparing the model to the vertical crystal sizes we should in principle take into account the vertical compression of crystals due to the ice flow. Had we chosen the horizontal crystal sizes for comparison, we should have taken into account the corresponding elongation. However, observations show that the crystal flattening, which is defined as crystal width divided by crystal height, is less than 15% for the applied samples (Svensson and others, 2003b), so in order to keep things reasonable simple, we simply ignore this effect.

During an annual cycle, the impurity content and the average crystal size show important

variations with the highest dust load and the smallest crystals appearing during spring (Svensson and others, 2003a). Because the size of the applied samples (20 cm depth) is close to the annual accumulation at NorthGRIP (19.5 cm ice equivalent), the seasonal variability will to a first order be averaged out in the experimental data. Still, some inter-annual variations in the impurity content of the ice are observed (Svensson and others, 2003a). These fluctuations may explain the small discrepancies between model and observations in Figs. 2 and 3, since the values of D and f are determined by the average concentration. We can take these fluctuations into account for the older samples, which have almost reached a steady state, by rescaling the crystal size distributions. In Fig. 4 we demonstrate that this rescaling results in a universal curve for all the size distributions, described by the steady state Bessel function solution, which is significantly different from the widely used log-normal distribution. The data-collapse in the figure, i.e. the fact that all the rescaled distributions have the same shape, clearly supports the one-parameter nature of the steady state solution (7).

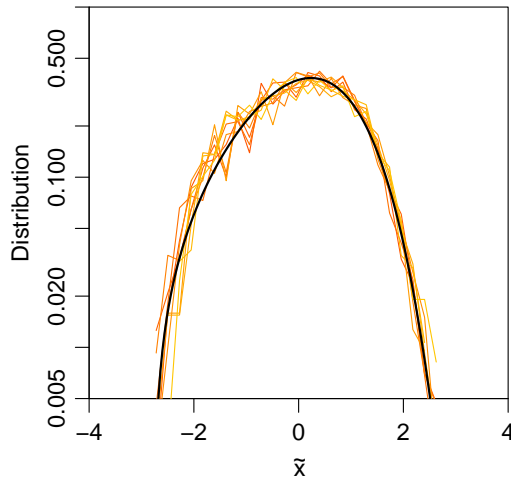


FIG. 4: The figure shows a “data collapse” of the size distributions as a consequence of a rescaling, $\tilde{x} = (\log x - \langle \log x \rangle) / \sigma(\log(x))$, i.e. the shown distributions have zero mean and unit standard deviation. The lines correspond to the eight data points in Fig. 3 of the oldest samples ($t > 2500$ years) and the black line on top is the steady-state solution of eq.(1). We use the rescaling \tilde{x} in order to improve the resolution around the smallest crystal sizes and note that the steady-state solution is transformed accordingly.

By formulating eq. (2) we thus provide a comprehensive description of the dynamical processes of ice crystals. Our model improves the Normal Grain Growth law based on diffusive growth alone and explains the reach of a steady state for the mean crystal size by means of fundamental physical processes. The very good agreement between data and model suggest that polygonization or fragmentation is the dominating process in production of small crystals rather than nucleation of new crystals, which is a process not included in the model. The suggested interplay between the diffusion and the fragmentation in the crystal dynamics is believed to be a central ingredient in many other systems in nature (like in geological and perhaps biological processes, see (Ferkinghoff-Borg and others, 2003)) and could provide a useful tool to predict the distribution curves of fragmented pieces.

-
- [1] Alley, R. B., J. H. Porepezko and C. R. Bentley. 1986. Grain growth in polar ice: II. application. *J. Glaciol.*, 32(112), 425-433.
 - [2] Alley, R. B., A. J. Grow and D. A. Meese. 1995. Mapping c-axis fabrics to study physical processes in ice. *J. Glaciol.*, 41(137), 197-203.
 - [3] Alley, R. B. and G. A. Woods. 1996. Impurity influence on normal grain growth in the GISP2 ice core. *J. Glaciol.*, 42(141), 255-260.
 - [4] Dahl-Jensen, D. and 6 others. 1998. Past temperatures directly from the Greenland ice sheet. *Science*, 282, 268-271.
 - [5] Dahl-Jensen, D. and 8 others. 2002. The NorthGRIP deep drilling program. *Ann. Glaciol.*, 35, 1-4.
 - [6] Li J., T. H. Jacka and V. Morgan. 1998. Crystal-size and microparticle record in the ice core from Dome Summit South, Law Dome, East Antarctica. *Ann. Glaciol.*, 27, 343-348.
 - [7] Ferkinghoff-Borg, J., M.H. Jensen, J. Mathiesen, P. Olesen and K. Sneppen. 2003. Competition between Diffusion and Fragmentation: An Important Evolutionary Process of Nature. *Phys. Rev. Lett.*, 91, 266103.
 - [8] Gow, A. J. and 6 others. 1997. Physical and structural properties of the Greenland Ice Sheet Project 2 ice core: A review. *J. Geophys. Res.*, 102(C12), 26,559-26,575.
 - [9] Johnsen, S. J. and 8 others. 2001. Oxygen isotope and palaeotemperature records from six Greenland ice-core stations: Camp Century, Dye-3, GRIP, GISP2, Renland and NorthGRIP.

Journal of Quaternary Science, 16(4), 299-307.

- [10] Paterson, W. S. B. 1994. *The Physics of Glaciers*, New York, Pergamon.
- [11] Svensson, A., P. Baadsager, A. Persson, C. S. Hvidberg and M.-L. Siggaard-Andersen. 2003a. Seasonal variability in ice crystal properties at NorthGRIP: A case study around 301m depth. *Ann. Glaciol.*, 37.
- [12] Svensson, A. and 6 others. 2003b. Properties of ice crystals in NorthGRIP late to middle Holocene ice. *Ann. Glaciol.*, 37.
- [13] Thorsteinsson, T., J. Kipfstuhl and H. Miller. 1997. Textures and fabrics in the GRIP ice core. *J. Geophys. Res.*, 102(C12), 26,583-26,599.
- [14] Wang, Y., T. Thorsteinsson, J. Kipfstuhl, H. Miller, D. Dahl-Jensen and H. Shoji. 2002. A vertical girdle fabric in the NGRIP deep ice core, North Greenland. *Ann. Glaciol.*, 35, 515-520.